Journal of Applied Polymer Science

Biodegradable Polyester Nanocomposites: Phase Miscibility and Properties

Vikas Mittal, Khalid Al Zaabi
Department of Chemical Engineering, The Petroleum Institute, Abu Dhabi, UAE
Correspondence to: V. Mittal (E-mail: vmittal@pi.ac.ae)

ABSTRACT: Melt mixing of poly(butylene adipate-co-terephthalate) based biopolymer was performed with synthetic silica and silicate reinforcements in order to attain nanocomposites with superior properties so as to enhance the spectrum of applications of the biopolymers. The addition of 5% of fillers enhanced the modulus of the polymer by 20% and also enhanced or retained the elongation and yield stress. The thermal properties of the polymer were unaffected by the addition of fillers and did not show any decrease in the degradation temperatures occasionally observed due to the acceleration of the degradation by heat accumulated in the filler aggregates. The morphological characterization of the composites confirmed good dispersion of filler particles in the polymer matrix, however, the magnitude of large sized aggregates increased with increasing filler fraction. The addition of filler also nucleated the polymer (peak crystallization temperature increased from 15 to 30°C) but the overall melt enthalpy was a function of filler dispersion. The dynamic properties of the composites enhanced gradually, however, significantly higher properties were observed for composites with 20% filler due to the presence of aggregates. An increase of storage modulus by 400% was observed for silica composites containing 20% filler, whereas same amount of silicate enhanced the storage modulus of the polymer by 300%. The composites with lower filler fractions maintained the similar flow characteristics as pure polymer. The filler phase was observed to be miscible with polymer in all composites except those with 20% filler content. © 2013 Wiley Periodicals, Inc. J. Appl. Polym. Sci. 000: 000–000, 2013

KEYWORDS: biomaterials; polyesters; rheology; thermal properties

Received 21 January 2013; accepted 20 February 2013; published online
DOI: 10.1002/app.39206

INTRODUCTION

Conventional nonbiodegradable polymers like polyolefins, polystyrene, poly(methyl methacrylate) and so forth, due to very challenging and costly recycling or reuse processes lead to accumulation of piles of nonbiodegradable wastes all over the world. Biodegradable polymers (biopolymers) have gained enhanced importance in the recent years due to increasing consciousness toward the use of more environmentally friendly materials, thus, shifting the focus from conventional nonbiodegradable polymers to "green" or biopolymers.[1] In a recent study by BCC Research, a significant compound annual growth rate (CAGR) of 22% for biodegradable polymers during the 5 year period starting from 2012 has been estimated.[2] However, most biopolymers have traditionally higher costs and inferior property profiles compared to commercial thermoplastic polymers, thus, requiring improvements to make them fully competitive. One such route is to generate bio-nanocomposites with enhanced properties as compared to the pure polymer.

Polymer nanocomposites are the hybrid materials in which at least one of the components has a dimension smaller than 100 nm. They offer an opportunity to explore new behaviors and functionalities beyond those of conventional materials. Nanoparticles, due to their small interparticle distances and the conversion of a large fraction of the polymer matrix near their surfaces into an interphase of different properties, often strongly influence the properties of the composites at very low volume fractions.[3] The nanocomposites can contain inorganic fillers falling into three different categories by the virtue of their primary particle dimensions.[4] When all the three dimensions of the particles are in the nanometer scale, the inorganic fillers have the form of spherical particles [zero-dimensional (0D)] like silica particles.[5,6] Fillers with two dimensions in the nanometer scale whereas the third one is in the range of micrometers include carbon nanotubes or whiskers (1D).[7,8] When two finite dimensions are in the range of micrometers, whereas the third dimension is in nanometer scale, the fillers include layered silicate (or aluminosilicate) materials (2D).[9] Incorporation of a large variety of fillers in the conventional polymers has been observed to cause significant enhancements in their mechanical, thermal, rheological and gas barrier properties.[5,10,11] In order to generate high value materials from biopolymers, similar nanocomposites

using fillers like layered silicates, nanotubes, and so forth, have also been reported.[12–14] This way, the biopolymers with improved properties with preservation of the material biodegradability without eco-toxicity could be achieved which have strong potential to replace the conventional polymers.

As mentioned above, a number of biopolymers have been reinforced with conventional fillers in order to generate bio-nanocomposites. Biopolymers are classified based on the biosynthesis or chemical synthesis processes as well as the origin of the monomers.[15] One such category corresponds to the polymers where both monomers and polymers are obtained by chemical synthesis from fossil resources, however, the obtained polymer is biodegradable. Prominent members of this category are poly(-butylene adipate-co-terephthalate) (PBAT) polymers, or generally named aromatic copolyesters. These polymers are aliphatic/aromatic copolyesters based on the monomers 1,4-butanediol, adipic acid and terephthalic acid. The general chemical structure of these materials is as follows (trade name Ecoflex® from BASF, Germany):

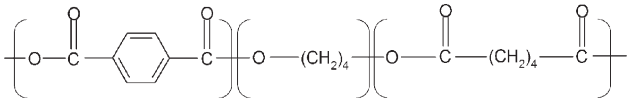

PBAT polymer has high flexibility than other biodegradable polyesters, such as poly(lactic acid) and poly(butylene succinate), therefore, has significant application for food packaging and agricultural flexible films. It was also confirmed from the biodegradation tests on the polymer that the polymer did not indicate any environmental risk (eco-toxicity) when introduced into composting processes.[16] Only a few studies reporting the composites of PBAT with nanofillers like layered silicates have been reported.[17–19] Chivrac et al. reported increase in the stiffness of the polymer as a function of clay (Cloisite 20A) content due to the strong interfacial interactions between the polymer and filler phases.[18] The nucleation of the polymer was also enhanced on addition of clay, but simultaneously crystal growth was hindered. Because of the immense commercial importance of PBAT polymers, it is important to further explore the nanocomposites of these materials with functional fillers like silica and silicate in order to access their suitability for various applications. Apart from mechanical performance, their thermal, rheological as well as morphological properties are also required to be analyzed in detail. The nanocomposites with silica (0-D) and alumino-silicate (2-D) are of particular interest because of their widespread use in commercial systems thus requiring no change in the processing technologies when generating these new class of biocomposites with PBAT polymers. Thus, generation of functional environmentally bio-nanocomposites adapted to existing processing technologies forms the motivation of the current study.

In this study, nanocomposites of PBAT polymer with 0-D and 2-D reinforcement phase were generated and analyzed for their properties. The phase miscibility was also studied as a function of filler fraction in the composites. The main goal of the study was to attain optimum enhancement in the properties of the pure polymer to enhance its application spectrum as well as to make the material competitive to the conventional nonbiodegradable polymers.

EXPERIMENTAL

Materials

Biopolyester with trade name Ecoflex® F Blend C1200 was supplied by BASF SE, Germany. It is a biodegradable aliphatic-aromatic copolyester based on the monomers 1,4-butanediol, adipic acid and terephthalic acid in the polymer chain, which biodegrades to the basic monomers and eventually to carbon dioxide, water and biomass when metabolized in the soil or compost under standard conditions. Synthetic silicon dioxide powder (ZEOFREE® 5161 S) and synthetic aluminium silicate (ZEOLEX® 23) were supplied by J. M. Huber Private Limited, India.

Generation of Bio-Nanocomposites

Bio-nanocomposites were prepared by melt mixing of the biopolymer with inorganic fillers using mini twin conical screw extruder (MiniLab HAAKE Rheomex CTW5, Germany). Mixing temperature of 140°C and rotational speed of 55 rpm were used and the mixing was performed for 7 min. The screw length and screw diameter were 109.5 and 5/14 mm conical respectively. Composites with filler content of 2, 5, 10, and 20% were generated. Pure polymer was also processed under same thermal conditions to maintain consistency. Disc and dumbbell-shaped test specimens for rheological and mechanical characterization were prepared by mini injection molding machine (HAAKE MiniJet II, Germany) at a processing temperature of 145°C. The injection pressure was 820 bar for 6 s whereas holding pressure was 400 bar for 3 s. The temperature of the mold was kept at 50°C.

Characterization of the Nanocomposites

Calorimetric properties of the pure polymer and bio-nanocomposites were recorded on a Netzsch Differential Scanning Calorimeter (DSC 200 F3 Maia) under nitrogen atmosphere. The scans were obtained from 50 to 170 to 50°C using heating and cooling rates of 15 and 5°C/min respectively. Thermal properties of the samples were analyzed using Netzsch Thermogravimetric Analyzer (STA 449 F1 Jupiter). Nitrogen was used as a carrier gas and the scans were obtained from 50 to 700°C at a heating rate of 20°C/min.

AR 2000 rheometer from TA Instruments was used to characterize rheological properties such as storage modulus (G'), loss modulus (G''), viscosity (η') and elasticity (η''). Disc shaped samples of 25-mm diameter and 2-mm thickness were characterized at 130°C using a gap opening of 1 mm. Frequency sweep scans (dynamic testing) of all polyester composites were recorded at 1% strain from $\omega = 0.1$ to 100 rad/s. Mechanical characterization of pure polymer and bio-nanocomposites was performed on universal testing machine (Testometric M350, UK). The dumbbell shaped samples with 53-mm length, 4-mm width, and 2-mm thickness were used. A loading rate of 5 mm/min was employed and the tests were carried out at room temperature. Win Test Analysis software was used for the calculation of tensile modulus and yield stress properties. An average of three values is reported.

For the bright field transmission electron microscopy analysis of the composite samples, Philips CM 20 (Philips/FEI, Eindhoven) electron microscope at 120 and 200 kV accelerating voltages was used. Thin sections of 70–90 nm thickness were microtomed

Table I. Tensile Properties of Bio-Polyester Nanocomposites as a Function of Filler Fraction

Composite	Modulus,[a] MPa	Yield stress,[b] MPa	Stress at break,[d] MPa	Elongation at yield,[c] mm
Pure polymer	77.7	9.1	20.9	2.9
2% silica	76.0	11.3	21.3	7.6
5% silica	91.0	11.0	20.7	5.1
10% silica	93.7	11.0	15.7	3.9
20% silica	63.5	11.9	14.3	3.2
2% silicate	79.1	8.4	21.8	5.2
5% silicate	92.0	9.2	19.3	5.2
10% silicate	90.1	8.0	16.4	1.4
20% silicate	77.7	6.2	14.0	1.8

[a]Relative probable error 5%.
[b]Relative probable error 2%.
[c]Relative probable error 5%.
[d]Relative probable error 15%.

from the sample block and were supported on 100 mesh grids sputter coated with a 3-nm thick carbon layer.

RESULTS AND DISCUSSION

The bio-polyester used in the study has transparent to translucent appearance and reported by the supplier to have semi-crystalline structure with melting point in the range of 110–120°C. The polymer has a combination of properties like flexibility, process ability, utilization properties, and biodegradability which are designed to meet the requirements of a biodegradable plastic. Typical applications are packaging films, agricultural films and compost bags, and so forth. It is generally reported that the generation of nanocomposites enhances the tensile modulus of the composites, but in return impacts the elongation negatively due to the presence of filler aggregates as well as strain hardening.[10] However, in order to retain the flexible film applications, it is required that the elongation of the polymer is not compromised for the modulus or viscosity enhancement.

Table I describes the tensile properties of the polyester nanocomposites. No significant effect on modulus was observed on addition of 2% silica and silicate fillers to the pure polymer. However, an increase of ~20% in the modulus was observed when the fraction of the fillers was enhanced to 5%. Also, the modulus was observed to reach an optimum as further increment in the filler fraction to 10% did not impact its magnitude significantly. At 20% filler content, the modulus was observed to decrease due to higher extent of filler in the matrix which in the absence of strong polymer-filler interfacial interactions would lead to stress concentration as well as large filler aggregates. This was also confirmed in the morphological characterization of the nanocomposites as shown in Figures 1 and 2. The dispersion of the silica and silicate filler particles was uniform in the nanocomposites, however, the magnitude and size of aggregates was observed to increase as the fraction of filler was enhanced. It should also be noted that the composites were generated without the addition of any commonly added low molecular weight comaptibilizer and still good filler dispersion (especially at lower fractions) could be achieved. The amphiphilic nature of common compatibilizers though leads to enhanced interactions between the filler and polymer phases, thus, resulting in better filler dispersion and delamination, however, owing to the low molecular weight, these compatibilizers are also observed to cause matrix plasticization along with reduction in crystallinity.[20,21] Yield stress of the silica nanocomposites was higher than the pure polymer and remained stable at all filler concentrations. The silicate composites, conversely, exhibited a decrease in the yield stress of the composites especially at high filler content, thus, indicating that the different structural morphology of the silica and silicate fillers resulted in different yield behavior. Because of the layered platelet morphology of the silicate particles, in which the platelets are held strongly in stacks by electrostatic forces between them, intercalation of polymer chains inside the platelet interlayers would constrain the polymer chains much more that the silica particles, where no such intercalation takes place. Filler surface modification by suitable modifier molecules which are compatible with the polymer structure can be expected to reduce the interlayer forces thus leading to enhanced filler dispersion. Elongation at yield for composites with 2% filler content was significantly higher than

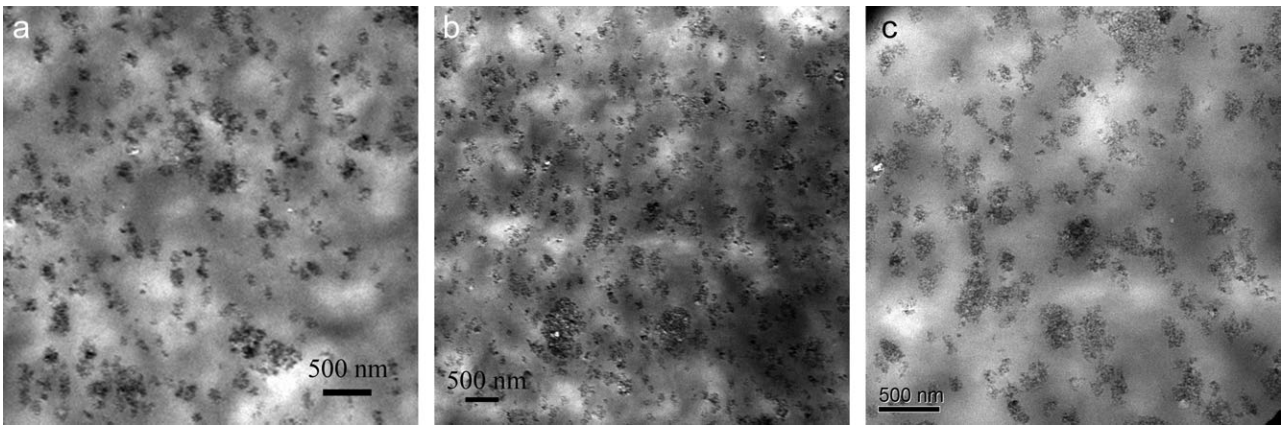

Figure 1. TEM micrographs of silica nanocomposites with different filler fractions: (a) 5%, (b) 10% and (c) 20%.

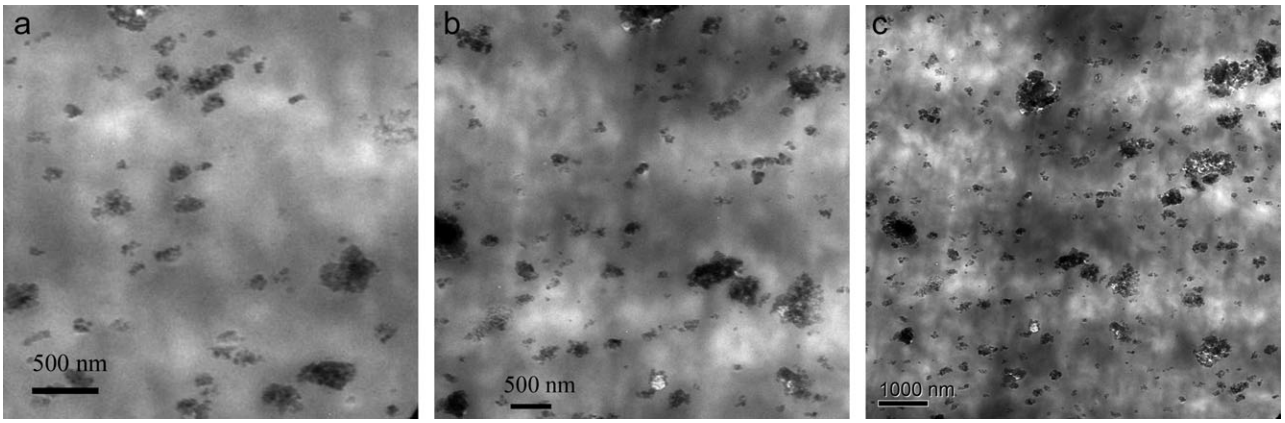

Figure 2. TEM micrographs of silicate nanocomposites containing different filler fractions: (a) 5%, (b) 10% and (c) 20%.

the pure polymer, which was retained when the filler fraction was enhanced to 5%. It indicated that the filler particles at lower filler content did not hinder the movement of the chains and their nano-scale dispersion even enhanced the toughness of the polymer. Further additions of filler decreased the elongation due to filler aggregates and strain hardening, however, silicate composites were more severely affected owing to above mentioned causes. It should also be noted that even by adding 20% filler in the polymer matrix, no observable change in the appearance of polymer occurred.

Figure 3 shows the TGA thermograms of the silica and silicate reinforced nanocomposites. In the nitrogen atmosphere, the peak degradation temperature of the polymer was observed to be 380°C. Addition of fillers did not impact the thermal degradation of polymer as the thermograms of the composites irrespective of filler type and amount were observed to overlap with each other, differing only in the extent of total weight loss. It was also earlier reported that the higher content of filler in the composites led to a decrease in the onset degradation temperature due to the accumulation of heat in the filler tactoids which accelerated the decomposition reaction.[19] However, no such phenomenon was observed for the composites in this study indicating that though the tactoids were present but their size was probably not large enough to induce the negative impact on thermal properties. Unlike thermal degradation behavior of the nanocomposites, the calorimetric properties of the nanocomposites, listed in Table II, were influenced by filler type as well as filler fraction. The peak crystallization temperature in the nanocomposites was observed at significantly higher temperatures than the pure polymer confirming that the filler particles nucleated the polymer crystallization (Figure 4). Addition of silicate (especially above 2%) exhibited much stronger nucleation than silica as the peak crystallization temperature in silicate composites increased by −30°C as compared to −15°C for silica composites. The peak melting point of the polymer did not show any significant variation and the magnitude remained within 2–3°C of the peak melting point of pure polymer (Figure 5). The melting transitions in the composites were broad and unsmooth particularly for silica containing nanocomposites. The melt enthalpy (corrected for actual polymer fraction in the composites) increased initially with filler fraction, but decreased afterwards. In silica composites, the decrease in melt enthalpy was observed after 5% filler fraction, whereas for the silicate composites, it was only 2%. Thus, even though the filler particles acted as nucleating agents for the polymer, the overall crystallinity decreased. Such a phenomenon was also reported earlier by Chivrac et al.,[19] where a small amount of

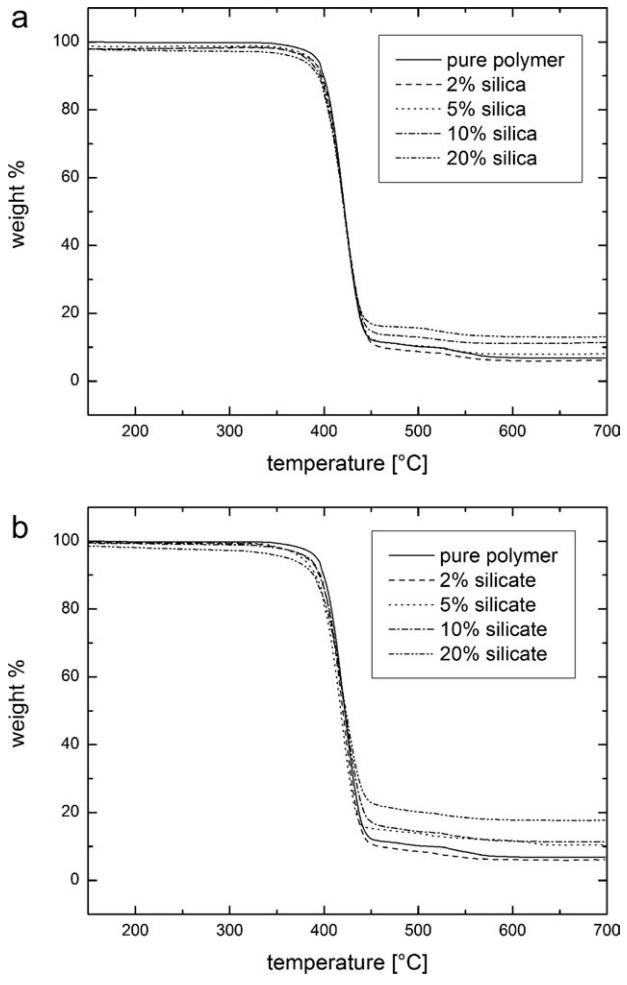

Figure 3. TGA thermograms of the silica and silicate nanocomposites as a function of filler fraction.

Table II. Calorimetric Properties of Polymer Nanocomposites with Silica and Silicate Fillers

Composite	T_m, °C	ΔH_m, J/g	T_c, °C
Pure polymer	123	12.4	71
2% silica	124	12.6	85
5% silica	121	14.6	84
10% silica	122	12.1	84
20% silica	123	11.3	85
2% silicate	122	15.4	88
5% silicate	122	14.0	100
10% silicate	120	12.7	100
20% silicate	124	11.9	99

silicate enhanced the nucleation of PBAT, but also hindered crystallite growth. In such cases, it was concluded that the state of filler dispersion impacted the resulting crystallization behavior and overall crystallinity. In the current study, the composites with higher extents of filler fraction were observed to have bigger sized aggregates, which would also justify dominance of crystallite growth hindrance over the nucleation effect of the filler particles thus leading to decrease in melt enthalpy. The composites with 10% filler content had melt enthalpy still similar to pure polymer, indicating that the nucleation effect still compensated for the hindrance to crystallite growth due to the filler aggregates.

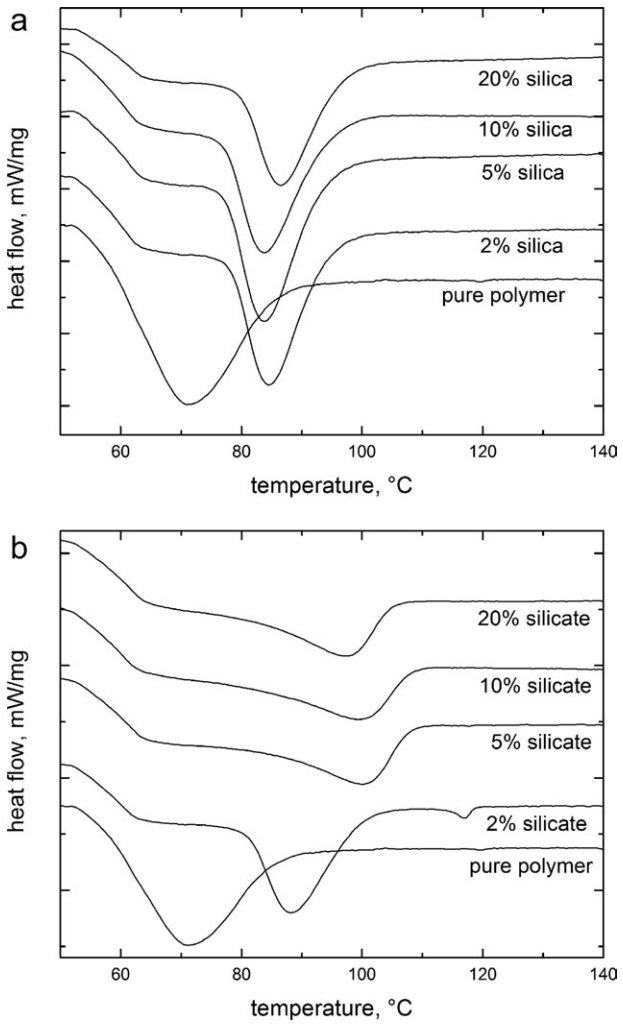

Figure 4. DSC crystallization thermograms of (a) silica and (b) silicate nanocomposites in comparison with pure polymer.

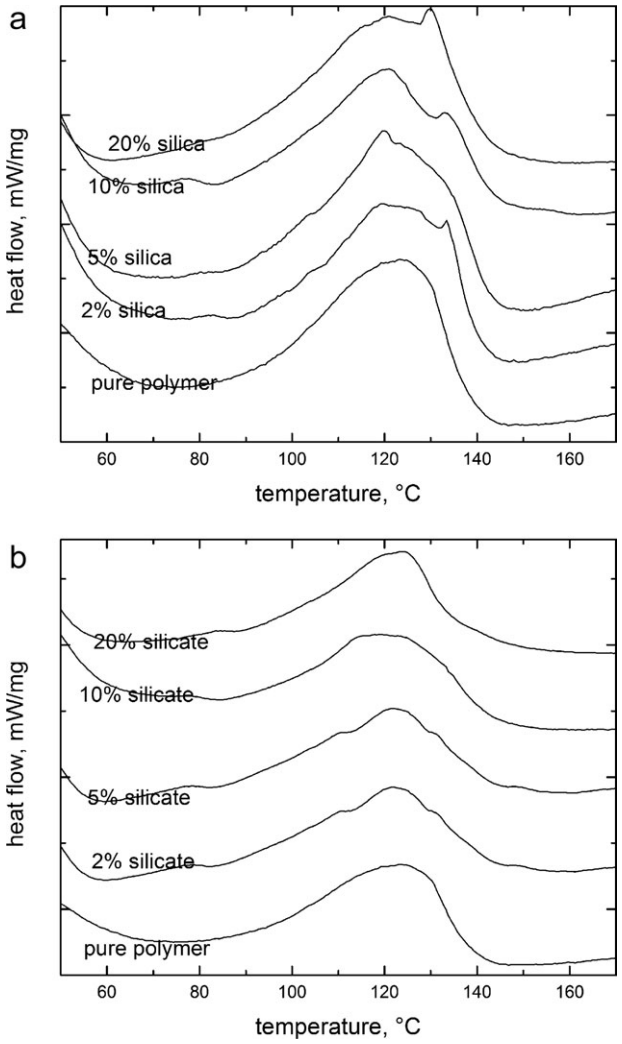

Figure 5. DSC melting thermograms of (a) silica and (b) silicate nanocomposites in comparison with pure polymer.

Storage modulus of the nanocomposites as a function of angular frequency is demonstrated in Figure 6. As the samples were observed to be safe up to 10% strain in the strain sweep run, frequency sweep of the samples was performed at a strain of 4% using frequency range of 0.1 to 100 rad/s. All the samples exhibited stability at low and high angular frequencies. In the case of silica nanocomposites, the storage modulus remained similar to the pure polymer till 5% filler fraction as shown in Figure 6(a) indicating that the composites exhibited similar flow properties as the pure polymer. Increasing further the amount of filler increased the storage modulus, thus, resulting in the highest values for the 20% silica containing composites. The

Applied Polymer SCIENCE

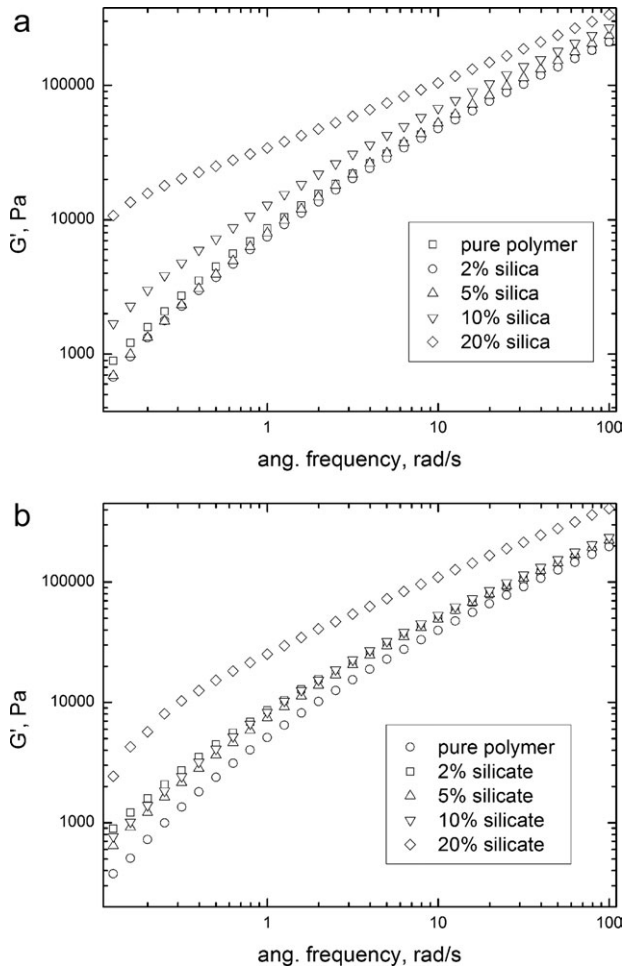

Figure 6. Storage modulus of the (a) silica and (b) silicate nanocomposites as a function of angular frequency and filler fraction.

20% composites had much higher modulus than the other composites especially at lower angular frequency values. For example, the shear modulus for pure polymer at an angular frequency of 1 rad/s was measured to be 8611 Pa which increased to 34,210 Pa for composite with 20% silica. The modulus curves approached each other at higher frequency values, thus, reducing the differences between the different samples and exhibiting concentration independent behavior. Figure 6(b) shows the similar curves for silicate nanocomposites. The values for 2, 5, and 10% composites were similar, however, they were higher than the pure polymer. The composite with 20% filler content had the highest modulus at all frequencies. For comparison, the shear modulus for 20% silicate nanocomposite at an angular frequency of 1 rad/s was measured to be 25,210 Pa. The curves overlapped at higher frequencies indicating concentration independence except for the composite with 20% filler. Owing to the presence of large filler aggregates (as confirmed earlier from the TEM micrographs), the storage modulus of 20% filler composites had much higher magnitudes. These findings were also reflected in oscillatory torque required to maintain the same strain in the samples during the rheological testing as shown in Figure 7. The torque required to strain the samples was maximum for 20% filler nanocomposites which resulted from the larger filler aggregates present in the polymer matrix. Similar to storage modulus, the loss modulus of the nanocomposites (Figure 8) also had gradual increase as compared to pure polymer till 10% filler fraction. The composites with 20% fraction had much higher modulus values especially at lower angular frequencies. For instance, at 1 rad/s angular frequency, loss modulus values of 31,000 and 38,010 Pa were observed for nanocomposites with 20% silica and silicate respectively, in comparison with 17,190 Pa for pure polymer.

Transition point from liquid like to solid like viscoelastic behavior is usually called gel point. At this point, polymer acts as true viscoelastic fluid. This behavior could be referred to the lesser molecular flexibility and mobility due to forming of viscoelastic gel or solid. Figure 9 shows these phenomena in relation with $\tan(\delta)$ versus angular frequency plot. For $\tan(\delta) > 1$, $G'' > G'$, whereas for $\tan(\delta) < 1$, $G'' < G'$. Thus, the above mentioned transition points can be recorded in Figure 9 at $\tan(\delta) = 1$. In pure polymer, $G'' > G'$ for all frequencies indicating the dominance of viscous component over the elastic part. The same was true for silica composites with 2 and 5% filler content. The composite with 10% filler content showed the

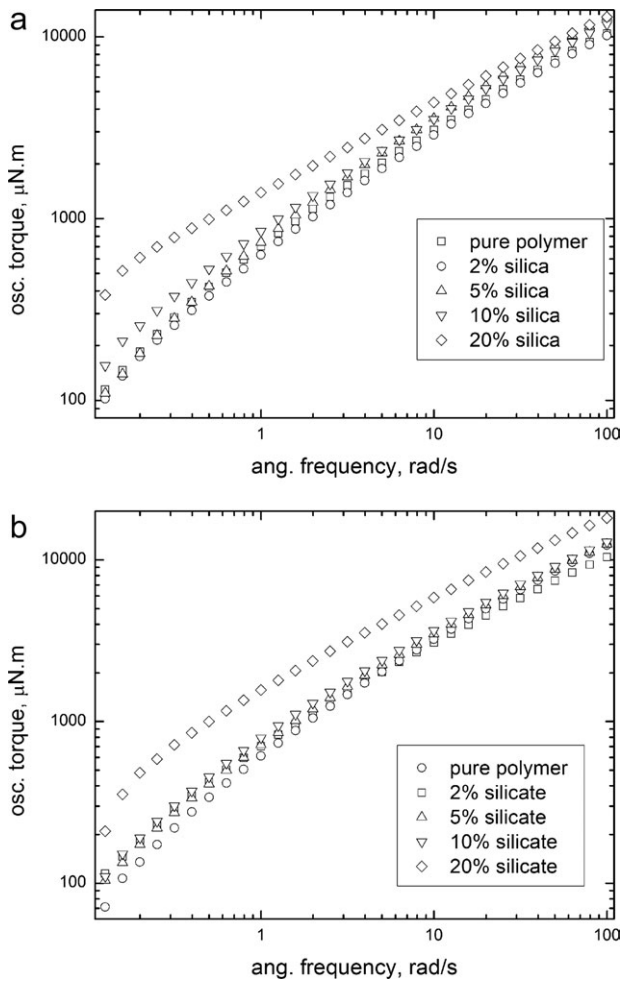

Figure 7. Oscillatory torque build-up as a function of filler fraction and angular frequency for (a) silica and (b) silicate nanocomposites.

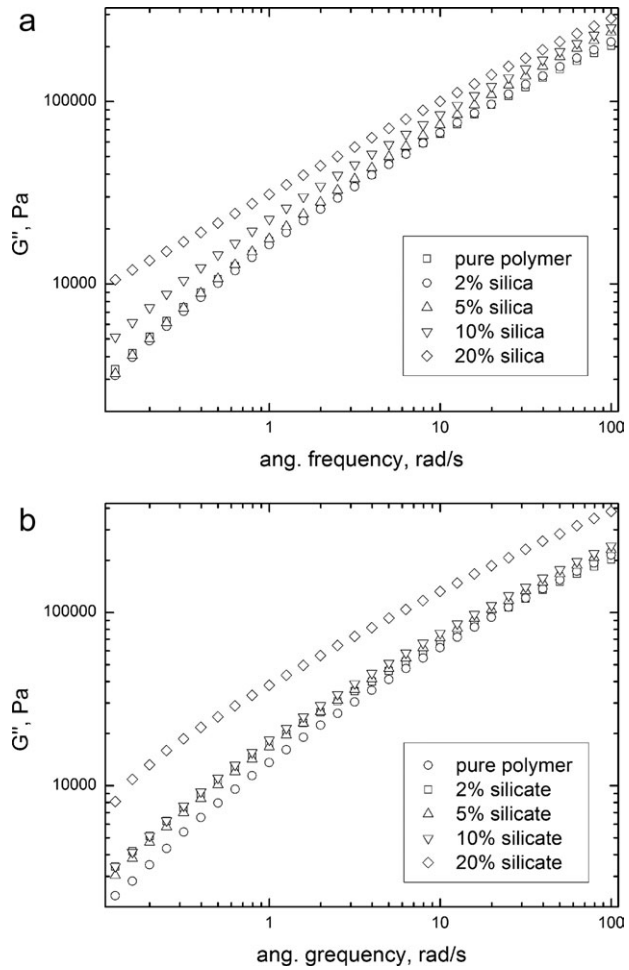

Figure 8. Loss modulus of the (a) silica and (b) silicate nanocomposites as a function of angular frequency and filler fraction.

transition from liquid like to solid like viscoelastic behavior at a frequency of 80 rad/s, whereas the transition was recorded at 0.13 rad/s for the 20% composite. It indicated that increasing the filler content also reinforced the elastic behavior of the polymer. In the corresponding silicate composites, the 20% filler composites showed the transition at 80 rad/s, whereas in other composites, viscous part was still dominant over the whole range of angular frequency. The different transition frequencies for the silica and silicate systems indicated that the behavior was impacted by the filler morphology which is further affected by the filler-polymer interactions as well as state of filler dispersion in the polymer.

Complex viscosity of the nanocomposites as a function of angular frequency is shown in Figure 10. The viscosity decreased on increasing angular frequency for all the samples. Similar to shear modulus, maximum value of complex viscosity was observed for nanocomposites containing 20% filler. At a frequency of 1 rad/s, the viscosity of the pure polymer was 19,220 Pa s which was increased to 46,170 and 45,610 Pa s in the case of nanocomposites with 20% silica and silicate respectively. The transition frequency between η' and η'' was also followed the same pattern as G' and G''. The curves for pure polymer and composites till 10% filler fraction approached each other at higher angular frequency, exhibiting reduced concentration dependence. However, the composites with 20% filler content had significant concentration dependent behavior even at higher angular frequency. It is also worth noting that the composites with even 10% filler fraction did not exhibit significant increase in viscosity thus maintaining the flow characteristics of the polymer.

The phase miscibility of the nanocomposites was studied using Cole–Cole viscosity plot which develops relationships between real (η') and imaginary (η'') parts of complex viscosity.[22–24] A smooth, semicircular shape of the graph would suggest miscible system with homogenous phase. The deviation from this behavior indicates phase segregation due to immiscibility of the components in the composites. As can be seen in Figure 11(a) for silica composites, composite with 20% silica content showed significant deviation from the semicircular shape indicating phase immiscibility probably due to the large filler aggregates present in the polymer matrix. Other composites exhibited a semicircular shape behavior indicating phase miscibility. In the

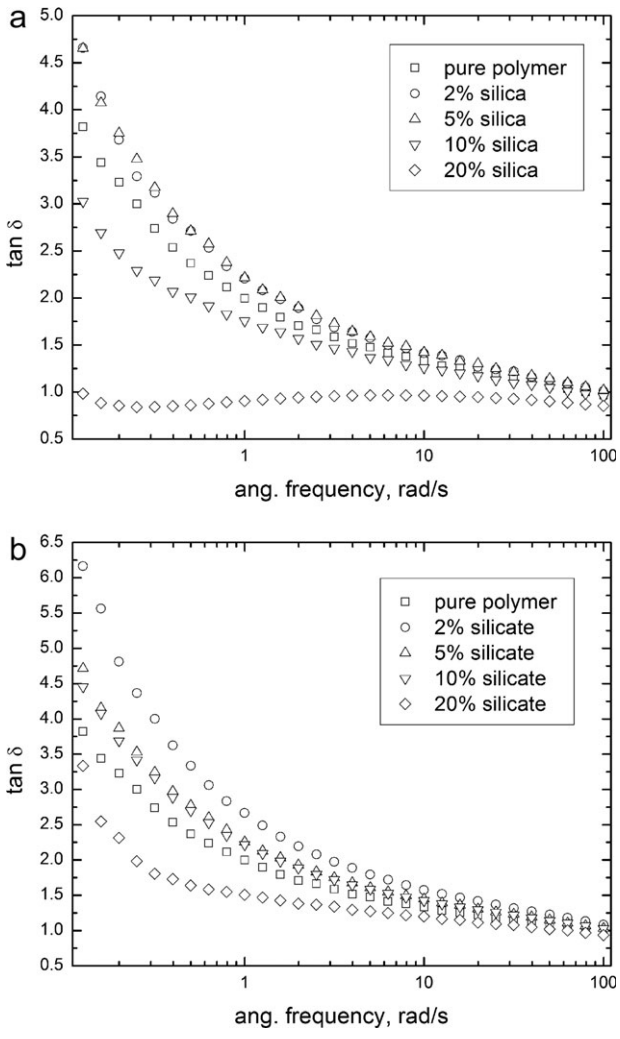

Figure 9. tan δ plot as a function of angular frequency for (a) silica and (b) silicate nanocomposites.

Applied Polymer SCIENCE

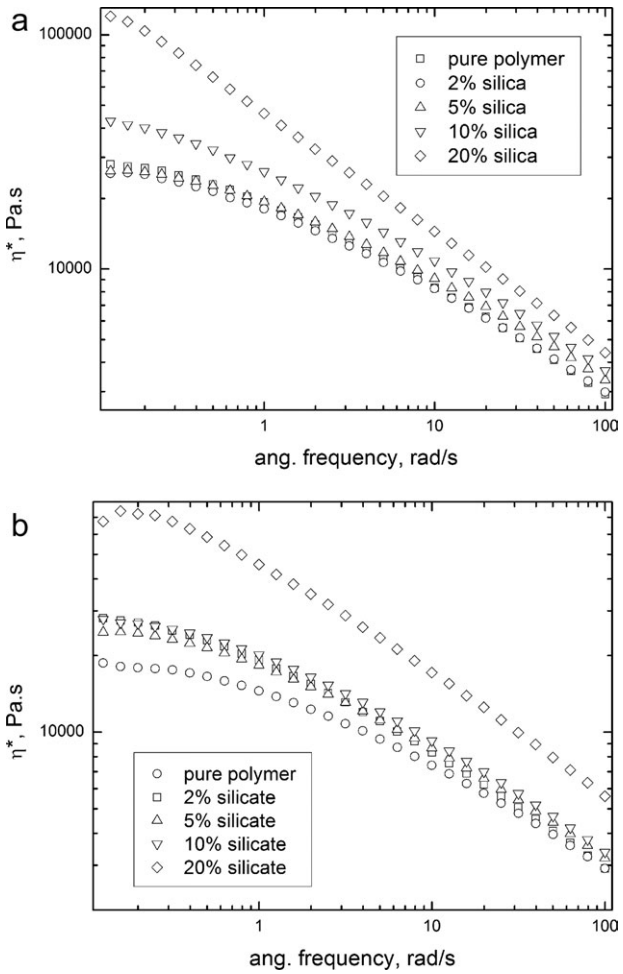

Figure 10. Complex viscosity of the (a) silica and (b) silicate nanocomposites as a function of filler fraction and angular frequency.

case of silicate nanocomposites depicted in Figure 11(b), the composite with 20% filler content did show deviation from semicircular path, especially at lower angular frequency, however, the extent of deviation was smaller than the corresponding silica composite. The other silicate composites exhibited well defined semicircular curves confirming phase miscibility in these systems. However, it is necessary to further support the findings from Cole–Cole plots as these findings could sometimes be misleading.[25]

Figure 12 shows the analysis of the rheological data based on van Gurp plots representing the relationship between complex modulus (G^*) and phase angle delta (δ).[26,27] The van Gurp plots confirmed the findings from Cole–Cole analysis. In the case of silica nanocomposites [Figure 12(a)], the time–temperature superposition principle was observed to hold (indicated by the merging of the curves into a common curve) for all the composites except the one with 20% filler. The deviation of the 20% filler containing composite was significant at lower frequency values. The silicate composites [Figure 12(b)] also exhibited closely approaching curves except for the composite with highest filler concentration. The magnitude of this exception was, however, not as large as the corresponding silica composite. It indicated that higher amounts of silicate filler may be better miscible with the polymer matrix in the applied processing conditions. It was earlier mentioned that the yield stress and elongation at yield of the silicate composites with higher extent of filler were inferior to the corresponding silica composites due to filler aggregates and strain hardening. However, the finding from the compatibility analysis of better phase miscibility in polymer-silicate system, it is likely that the strain hardening contributed primarily to the reduction in yield properties.

The phase miscibility of the nanocomposites was also analyzed using criteria reported for compatibility by Han and Chuang[28,29] as shown in Figure 13. When G' is plotted vs G'', such analysis generates composition independent correlation for compatible systems, whereas the correlation is composition dependent for incompatible systems. For silica composites [Figure 13(a)], concentration independent correlation was observed for composites except for 20% filler composite. This behavior was significant especially at lower angular frequency and approached the common curve at higher values of frequency. Thus, these findings confirmed the phase immiscibility of the system at

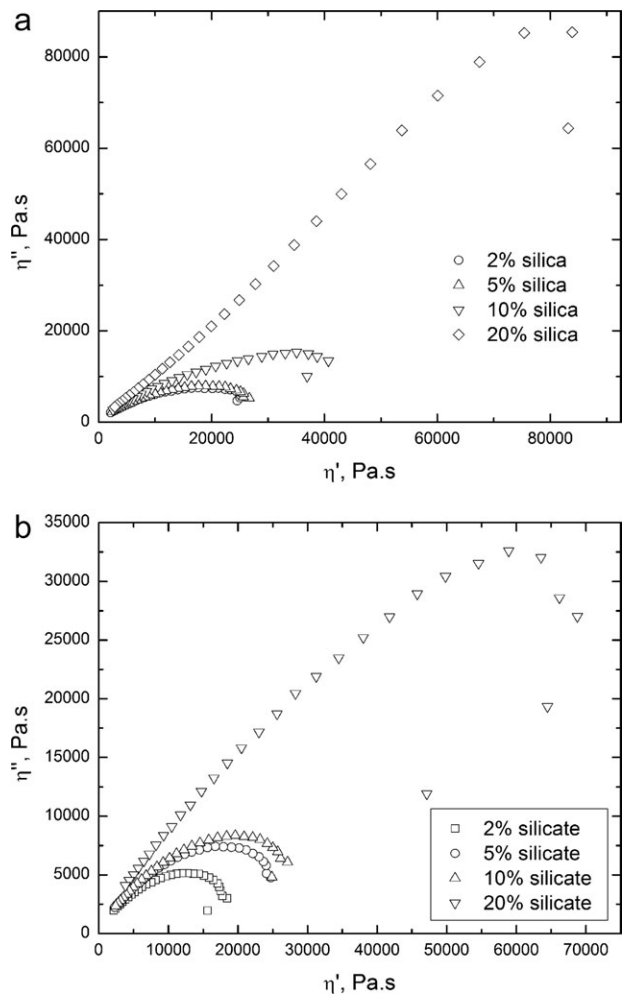

Figure 11. Cole–Cole plots of (a) silica and (b) silicate nanocomposites for assessing phase miscibility.

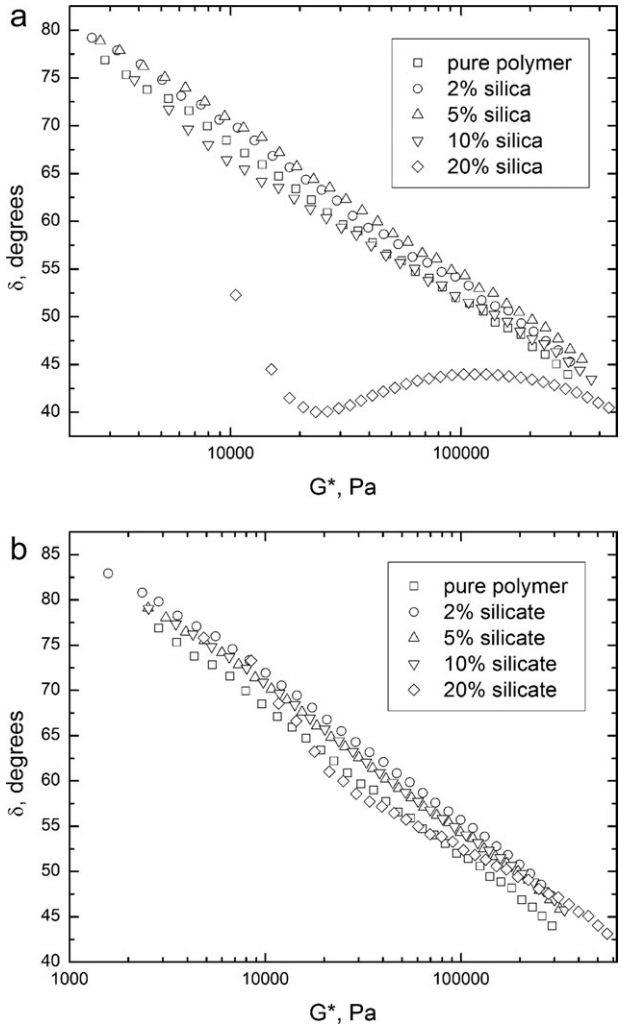

Figure 12. van Gurp plots of (a) silica and (b) silicate nanocomposites for component viscosity analysis.

higher silica content. The silicate nanocomposite with 20% silicate fraction though showed slight deviation from the common curve [as shown in the extended region of Figure 13(b)], however, the miscibility was better than the corresponding silica composite. These findings fully correlated with the earlier analysis using Cole–Cole plots as well as van Gurp plots and confirmed that the addition of 20% filler to the polymer in general deteriorated the mechanical performance, but in comparison, the silicate filler was still more miscible than the silica particles.

CONCLUSIONS

In the current study, nanocomposites of PBAT bio-polyester with silicon dioxide and aluminium silicate were generated with an aim to enhance the potential of the biopolymer to replace the conventional nonbiodegradable polymers for various applications. Addition of 5% of the filler enhanced the tensile modulus of the polymer by 20%. Further addition of the filler did not enhance the composite modulus. The characteristic elongation of the polymer increased till 5% filler fraction in the composites (>5 mm for composites as compared to 2.9 mm for pure polymer) and the yield stress was also enhanced or remained unaffected. At higher concentrations of filler, the silicate containing composites were observed to have reduction in both yield stress as well as elongation due to the strain hardening. Large sized aggregates were also observed in the TEM micrographs of the silica and silicate composites with higher extent of filler fraction. The filler particles acted as strong nucleating agents for the pure polymer, however, the melt enthalpy decreased after initial increase as a function of filler fraction. Thus, the filler aggregation at higher filler concentration hindered the crystal growth. The dynamic modulus and viscosity of the 20% filler containing composites (300–400% increase in storage modulus and 250% increase in complex viscosity) was observed to be significantly higher than pure polymer as well as other composites probably due to the presence of aggregates which also exhibited a similar increase in the oscillatory torque required to strain the samples during rheological testing. The composites with lower filler fractions did not exhibit significant modification of the polymer flow characteristics thus allowing the use of similar processing protocols during commercial processing. The composites exhibited dominant viscous behavior at lower filler contents, however the transition from liquid to viscoelastic gel was impacted by filler morphology. The

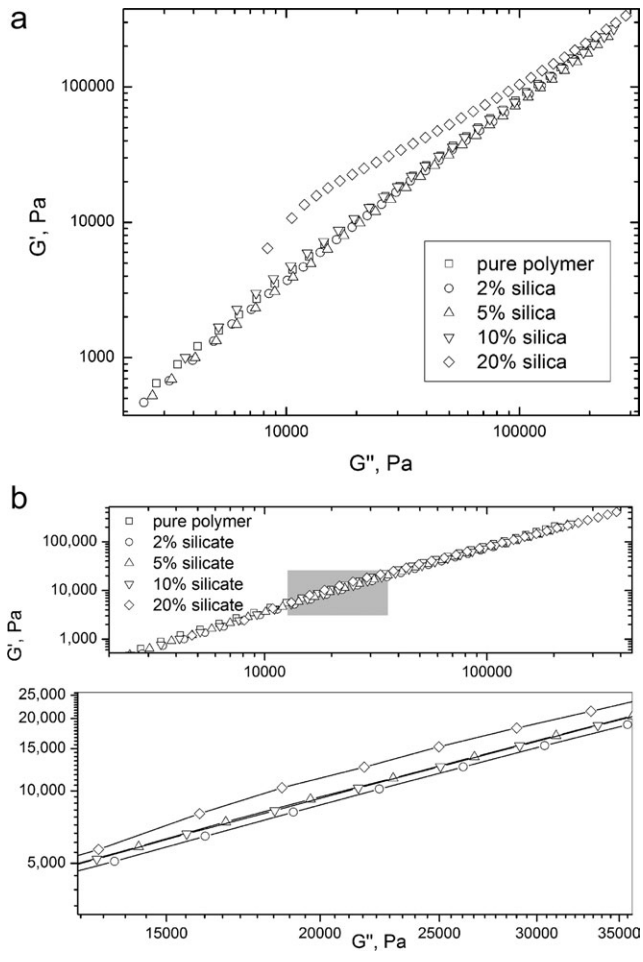

Figure 13. Han-Chuang (G' and G'') plots of (a) silica and (b) silicate nanocomposites.

miscibility analysis also revealed phase immiscibility in 20% filler composites, the magnitude of which was much higher in silica nanocomposite.

ACKNOWLEDGMENTS

The authors are indebted to Dr. N. B. Matsko at Graz Centre for Electron Microscopy, Austria for the microscopy analysis.

REFERENCES

1. Bordes, P.; Pollet, E.; Avérous, L. *Prog. Polym. Sci.* **2009**, *34*, 125.
2. BCC Research Report, Biodegradable Polymers, PLS025C, December 2007. (Available at: http://www.bccresearch. com/report/biodegradable-polymers-market-pls025d.html).
3. Brechet, Y.; Cavaille, J. Y.; Chabert, E.; Chazeau, L.; Dendievel, R.; Flandin, L.; Gauthier, C. *Adv Eng Mater*, **2001**, *3*, 571.
4. Pavlidoua, S.; Papaspyrides, C. D. *Prog. Polym. Sci.* **2008**, *33*, 1119.
5. Mark, J. E. *Polym. Eng. Sci.* **1996**, *36*, 2905.
6. Reynaud, E.; Gauthier, C.; Perez, J. *Rev. Metall. Cah. Inf. Tech.* **1999**, *96*, 169.
7. Calvert, P. In Carbon Nanotubes; Ebbesen, T. W., Ed.; CRC Press: Boca Raton, FL, USA, **1997**; pp. 277.
8. Favier, V.; Canova, G. R.; Shrivastava, S. C.; Cavaille, J. Y. *Polym. Eng. Sci.* **1997**, *37*, 1732.
9. Mittal, V. Organic Modifications of Clay and Polymer Surfaces for Specialty Applications; PhD Thesis, ETH Zurich: Zurich, Switzerland, **2006**.
10. Mittal, V. *J. Thermoplast. Compos. Mater.* **2007**, *20*, 575.
11. Chaudhry, A. U.; Mittal, V. *Polym. Eng. Sci.* **2013**, *53*, 78.
12. Ray, S. S.; Yamada, K.; Okamoto, M.; Ueda, K. *Polymer* **2003**, *44*, 857.
13. Sinha Ray, S.; Bandyopadhyay, J.; Bousmina, M. *Polym. Degrad. Stab.* **2007**, *92*, 802.
14. Favier, V.; Canova, G. R.; Shrivastava, S. C.; Cavaille, J. Y. *Polym. Eng. Sci.* **1997**, *37*, 1732.
15. Averous, L.; Boquillon, N. *Carbohydr. Polym.* **2004**, *56*, 111.
16. Witt, U.; Einig, T.; Yamamoto, M.; Kleeberg, I.; Deckwer, W.-D.; Muller, R. J. *Chemosphere* **2001**, *44*, 289.
17. Someya, Y.; Sugahara, Y.; Shibata, M. *J. Appl. Polym. Sci.* **2005**, *95*, 386.
18. Chivrac, F.; Kadlecova, Z.; Pollet, E.; Averous, L. *J. Polym. Environ.* **2006**, *14*, 393.
19. Chivrac, F.; Pollet, E.; Averous, L. *J. Polym. Sci. Part B: Polym. Phys.* **2007**, *45*, 1503.
20. Mittal, V. *J. Appl. Polym. Sci.* **2008**, *107*, 1350.
21. Chaudhry, A.U.; Mittal, V. *Polym. Eng. Sci.*, to appear.
22. Cho, K.; Lee, B. H.; Hwang, K. M.; Lee, H.; Choe, S. *Polym. Eng. Sci.* **1998**, *38*, 1969.
23. Kim, H. K.; Rana, D.; Kwag, H.; Choe, S. *Korea Polym. J.* **2001**, *8*, 34.
24. Kwag, H.; Rana, D.; Choe, K.; Rhee, J.; Woo, T.; Lee, B. H.; Choe, S. *Polym. Eng. Sci.* **2000**, *40*, 1672.
25. Utracki, L. A. Rheology of Polymer Alloys and Blends; Hanser Publishers: Munich, **1989**.
26. Joshi, M.; Butola, B. S.; Simon, G.; Kukaleva, N. *Macromolecules* **2006**, *39*, 1839.
27. van Gurp, M.; Palmen, J. *Rheol. Bull.* **1998**, *67*, 5.
28. Chuang, H. K.; Han, C. D. *J. Appl. Polym. Sci.* **1984**, *29*, 2205.
29. Han, C. D.; Chuang, H. K. *J. Appl. Polym. Sci.* **1985**, *30*, 4431.